ELSEVIER

International Journal of Mass Spectrometry 192 (1999) 125–139

International Journal of Mass Spectrometry

Redox properties of charged and neutral iron chlorides $FeCl_m^n$ (m = 1–3; n = −1, 0, +1, and +2)

Detlef Schröder*, Susanne Bärsch, Helmut Schwarz

Institut für Organische Chemie der Technischen Universität Berlin, Straße des 17. Juni 135, D-10623 Berlin, Germany

Received 18 December 1998; accepted 10 March 1999

Abstract

Electron transfer in high-energy collision experiments is used to probe the redox chemistry of the iron chlorides $FeCl_m^n$ (m = 1–3; n = −1, 0, +1, and +2). These experiments comprise charge inversion of $FeCl_m^-$ anions (m = 2–4) to cations, charge inversion of $FeCl_m^+$ cations (m = 1–3) to anions, charge stripping of $FeCl_m^+$ monocations (m = 1–3) to dications, and charge exchange of $FeCl_m^{2+}$ dications (m = 1, 2) to monocations. Ab initio calculations at the B3LYP/6-311+G* level of theory are used to evaluate the differences between adiabatic and vertical electron transfers; the accuracy of the calculated absolute energies for the associated electron-transfer processes predicted at this level of theory is doubted, however. The experimentally determined redox properties of the iron chlorides are in fair agreement with literature thermochemistry; new data derived in this work are: IE($FeCl_3$) = 10.9 eV, IE($FeCl^+$) = 15.9 ± 0.4 eV, IE($FeCl_2^+$) = 17.6 ± 0.7 eV, and IE($FeCl_3^+$) = 16.0 ± 0.4 eV. In addition, evidence for the existence of the chlorine complexes $Fe(Cl_2)^+$ and $Fe(Cl_2)^{2+}$ is presented. According to the experimental data, diatomic $FeCl^{2+}$ is a thermochemically stable dication, whereas $FeCl_2^{2+}$ and $FeCl_3^{2+}$ are metastable with respect to the dissociations into $FeCl_{(m-1)}^+ + Cl^+$ and $FeCl_{(m-2)}^+ + Cl_2^+$ (m = 2, 3). Except for the dications, the dissociation behavior of the $FeCl_m^n$ species (m = 1–3; n = −1, 0, +1) is dominated by sequential losses of chlorine atoms rather than expulsion of molecular chlorine. (Int J Mass Spectrom 192 (1999) 125–139) © 1999 Elsevier Science B.V.

Keywords: B3LYP calculations; Charge inversion; Charge stripping; Electron transfer; Iron chlorides; Redox properties

1. Introduction

Iron chlorides are important in geochemical processes, ore refinery, and corrosion. In particular, ferrous chloride $FeCl_3$ serves as a valuable single-electron oxidant, which is used in several synthetic procedures as well as numerous applied processes, e.g. the etching of copper in the manufacture of electronic devices. The gas-phase properties of ferric and ferrous chloride have been studied quite extensively by experimental and theoretical methods [1–6]. Recently, some comprehensive studies of the thermochemistry of iron chlorides have been published [7–11], and a survey of the present knowledge on the $FeCl_m^n$ system (m = 1–3; n = −1, 0, +1) is given in Table 1.

Here, we report a study of the redox properties of iron chlorides in the gas phase by examining electron transfer occurring in high-energy collisions using tandem mass spectrometry. The methods comprise collisional activation (CA), charge reversal (CR) of anions to cations and vice versa, neutralization reionization (NR), charge stripping (CS) of mono- to

* Corresponding author. E-mail: df@www.chem.tu_berlin.de

PII S1387-3806(99)00094-9

Table 1
Adiabatic electron affinities (EA_a, eV), adiabatic ionization energies (IE_a, eV) of $FeCl_m$ ($m = 1–3$) and the respective bond dissociation energies (eV) $D_0(Fe–Cl^-)$ of the anionic, $D_0(Fe–Cl)$ of the neutral, and $D_0(Fe^+–Cl)$ of the cationic iron chlorides. For the sake of consistency, all values were taken from a recent theoretical study [8] at the QCISD level of theory that agrees favorably with experimental literature data

	EA_a	IE_a	$D_0(Fe–Cl^-)$	$D_0(Fe–Cl)$	$D_0(Fe^+–Cl)$
FeCl	1.54	7.89	1.58	3.55	3.45
$FeCl_2$	0.99	10.10	2.23	4.74	2.52
$FeCl_3$	3.90		2.97	2.55	

dications, and charge exchange (CE) of di- to monocations. Energy-resolved measurements allow us to extract the energy demands of the associated vertical electron-transfer processes. In order to compare the experimental data with the literature thermochemistry of iron chlorides, theoretical methods employing the B3LYP hybrid functional are used to estimate the relevant differences between the adiabatic and vertical electron-transfer processes involved.

2. Experimental methods

The experiments were performed with a modified VG ZAB/HF/AMD 604 four-sector mass spectrometer of BEBE configuration that has been described elsewhere [12]. The two magnetic [B(1) and B(2)] and two electrostatic [E(1) and E(2)] sectors allow for separation and analysis of the ions of interest. Collision cells in the field-free regions enable us to perform different experiments. The following methods were applied for ion generation: (1) $FeCl_m^-$ anions ($m = 2–4$) were produced by either electron ionization (EI) of gaseous $FeCl_3$ or by chemical ionization (CI) of a ~1:10 mixture of $Fe(CO)_5$ and molecular chlorine. Despite its significant electron affinity (Table 1), the monochloride anion $FeCl^-$ was observed only in very minor amounts, which did not suffice to conduct any further experiments. Similarly, the yields for $FeCl_2^-$ only allowed for energy-resolved charge reversal of the parent ion. (2) $FeCl_m^+$ cations ($m = 1–3$) were made using the same methods (i.e. EI of $FeCl_3$ or CI of $Fe(CO)_5/Cl_2$) in the positive ion mode. (3) $FeCl_m^{2+}$ dications ($m = 1, 2$) were generated by EI of $FeCl_3$ at electron energies exceeding 30 eV. After acceleration by an 8 kV voltage, the ions were mass selected with the magnetic and electric sectors indicated below and subjected to collision experiments at variable transmissions (T). Due to natural isotope abundances, the mass spectra of $^{56}Fe^{35}Cl_m^n$ species ($m = 1–4$; $n = -1, +1, +2$) always contain some $^{54}Fe^{37}Cl^{35}Cl_{(m-1)}^n$ as shown by signals due to $^{54}Fe^+$, $^{37}Cl^-$, etc. Other isobaric interferences as well as $Fe_2Cl_{2m}^{2+}$ were negligible, and all $FeCl_m^n$ species ($m = 1–4$; $n = -1, +1, +2$) under study showed the expected isotope patterns. The mass spectra were obtained with the respective sectors following the collision cell(s) used, on-line processed, and accumulated using the AMD/Intectra data system. Due to hardware limitations of the digitizer, the energy-resolved experiments were acquired as repetitive single scans using an x/y recorder in order to maintain the full energy resolution of the instrument. Unfortunately, both EI of $FeCl_3$ and CI of $Fe(CO)_5/Cl_2$ are associated with serious contamination of the ion source resulting in a considerable decrease of the instrument performance, which requires frequent cleaning, including complete disassembly of the ion source. Therefore, not all experiments conceivable with $FeCl_m^n$ ions were conducted.

All species generated in the ion source were characterized by collisional activation of the B(1)/E(1) mass-selected ions using helium (80% T) as collision gas. In addition, the B(1)/E(1) mass-selected $FeCl_m^-$ anions ($m = 3, 4$) were examined by charge reversal ($^-CR^+$ [13], O_2, 80% T) and neutralization reionization ($^-NR^+$ [14], O_2/O_2, 80% T/80% T) experiments. Quantitative comparison of the $^-CR^+$ and $^-NR^+$ spectra in terms of the recently developed

NIDD scheme (NIDD, neutral and ion decomposition difference [15,16]) provided information about the behavior of the transient neutral iron chlorides formed in these experiments. In this scheme, subtraction of the intensities measured in the $^{-}CR^{+}$ mass spectrum from those intensities observed in the $^{-}NR^{+}$ experiment results in a difference spectrum that permits one to trace back the contributions of the neutral transient species. Further, $^{+}NR^{+}$ ([14]; Xe/O_2, 80% T/80% T), and charge stripping (CS [17], O_2, 80% T) spectra of the B(1)/E(1) mass-selected $FeCl_m^+$ cations (m = 1–3) were recorded using B(2). The $FeCl_m^{2+}$ dications (m = 1, 2) produced in the ion source were also examined by charge exchange (CE [18], He and O_2, 80% T) of the B(1)/E(1) mass-selected ions to the corresponding monocations as well as charge stripping (He, Ne, and O_2, 50–80% T) to possibly afford trications [19,20]. Due to low intensities, only the recovery signals of the B(1) mass-selected precursor cations were examined in the $^{+}CR^{-}$ (Xe, 60% T) and $^{+}NR^{-}$ (Xe/Xe, 80% T/80% T) experiments.

Because of the superior energy resolution of E(1), the energy-resolved experiments were performed with B(1)-only mass-selected ions [21]. Note that parent selection using a single sector may give rise to artifact peaks [22], although we found no indications for these in the present set of experiments. In order to quantitatively analyze the energy demands of the electron-transfer processes involved, the parent and recovery ions in charge-reversal and charge-stripping experiments were scanned at energy resolutions $E/\Delta E$ of ~5000 in conjunction with appropriate calibration schemes (see below). In the net balance, $^{-}CR^{+}$, $^{+}CR^{-}$, and CS are all endothermic processes, and the energies required are provided by the translational energies of the keV projectiles, thereby giving rise to a decrease of the ions' kinetic energies. To a first approximation [21,23], these energy balances can be described as follows: (1) In $^{-}CR^{+}$, the energy difference $\Delta E_{^{-}CR^{+}}$ corresponds to the removal of two electrons from a polyatomic anion A^-, i.e. the vertical transition $A^- \rightarrow A^+$. It is obvious that $\Delta E_{^{-}CR^{+}} \geq EA_a(A) + IE_a(A)$, i.e. the sum of the adiabatic electron affinity (EA_a) and the adiabatic ionization energy (IE_a), because the cation formed upon vertical two-electron oxidation of the anion is generally not formed at the equilibrium geometry of A^-. (2) The corresponding energy balance $\Delta E_{^{+}CR^{-}}$ is composed of the energy gain upon addition of two electrons to a cation A^+ and the energy loss by removal of two electrons from the target, here xenon [23–25]. There are two conceivable scenarios for the removal of the two electrons in the $^{+}CR^{-}$ process. The first situation is a stepwise electron transfer, i.e. $A^+ + 2\,T \rightarrow A^- + 2\,T^+$, where the necessary excess energy is provided by the kinetic energy of the projectile. Thus, the minimum value of $\Delta E_{^{+}CR^{-}}$ corresponds to $2 \cdot IE(Xe)$ = 24.26 eV minus the energy gained in the vertical transition $A^+ \rightarrow A^-$. Due to geometry differences of the associated vertical transitions, the term 24.26 eV $- \Delta E_{^{+}CR^{-}}$ would therefore be expected to be equal or smaller than the sum of EA_a and IE_a. The second scenario corresponds to a direct transfer of two electrons in a single collision, i.e. $A^+ + T \rightarrow A^- + T^{2+}$ [25,26]. However, this process would appear at much lower kinetic energies than the high-energy onset of the recovery signal because of sequential electron transfer, because $2 \cdot IE(T) \ll IE(T) + IE(T^+)$; here, $2 \cdot IE(T)$ = 24.26 eV compared to the energy demand of 33.43 eV for double ionization of xenon. (3) The kinetic energy deficit of dications formed in CS, usually referred to as Q_{min} value [27], roughly corresponds to the vertical ionization energy of the monocation $IE_v(A^+)$. All these energy deficits can be determined from the high-energy onsets of the precursor ion and the corresponding recovery ion beams, provided appropriate calibration schemes are employed. The values given below refer to the average of at least three different experiments, and the errors given comprise the standard deviation of the measured energy balances as well as systematic errors of the associated calibration schemes. Note that these measurements are sensitive to accidental changes in the ionization conditions (discharges in particular) because they require the constancy of the absolute ion kinetic energies. Therefore, we recommend the exclusion of any set of data in which serious changes of the ion's kinetic energies occur (either for the ions of interest or the references).

As demonstrated previously, there may exist sig-

nificant differences between the energy deficits for a single two-electron transfer in one collision cell, i.e. ΔE_{CR}, versus double single-electron transfer in two consecutive collision cells with intermediate selection of the neutral species, i.e. ΔE_{NR} [25,28]. However, for the iron chlorides examined here the high-energy onsets of the recovery ions in the energy-resolved CR and NR spectra were identical within the experimental error (±0.3 eV) in the direct comparison of the measurements. Therefore, we shall only refer to the more sensitive CR experiments.

The following electron-transfer processes were used in the calibration of the respective energy scales: (1) charge inversion of halide ions $X^- \rightarrow X^+$ (X = F, Cl, Br, I) and $O_2^- \rightarrow O_2^+$ for $^-CR^+$ [21,25,28], (2) charge inversion of the halogen cations $X^+ \rightarrow X^-$ for (X = Cl, Br, I) as well as $O_2^+ \rightarrow O_2^-$ for $^+CR^-$ [23–25,28], and (3) charge stripping of the molecular ion of toluene, $C_7H_8^+ \rightarrow C_7H_8^{2+}$, with $Q_{min}(C_7H_8^+)$ = 15.7 eV [18,27]. Note that the calibration schemes for CR used several references, whereas the energy scale of CS relies on Q_{min} ($C_7H_8^+$) as a single anchor.

3. Theoretical methods

The thermochemistry of $FeCl_m^n$ (m = 1–3; n = −1, 0, +1 except for $FeCl_3^+$) has recently been treated comprehensively by Bach et al. [8], who applied a range of theoretical levels including density functional methods (see also [9], [10]). Rather than providing a more complete set of accurate ab initio thermochemical data for $FeCl_m^n$ (m = 1–3; n = −1, 0, +1, +2), the primary aim of our theoretical investigation was the assessment of the differences between the vertical electron transfers sampled in the mass-spectrometric experiments and the corresponding adiabatic processes. Therefore, we applied the B3LYP functional implemented in GAUSSIAN94 together with 6-311+G* basis sets [29]. Clearly, this level of theory cannot provide highly accurate predictions of thermochemical properties, but it is expected to provide reasonable descriptions of $FeCl_m^n$ (m = 1–3; n = −1, 0, +1) within about ±0.5 eV uncertainty (see below). Moreover, the accuracy of relative energies within the potential-energy surface of a given species is much better, and therefore, this level of theory is deemed to be adequate for converting the experimentally measured vertical energy deficits to the corresponding adiabatic processes.

In general, in our calculations we used as inputs the geometries and states reported by Bach et al. [8], followed by full geometry optimizations and frequency calculations. Note, however, that one cannot exclude that there may exist other states of the species studied (either in symmetry or in multiplicity [9]), which are even lower in energy; in fact, B3LYP may not be an appropriate level of theory in this respect [30]. However, the use of B3LYP for the estimation of the differences between vertical and adiabatic electron transfers appears appropriate, given the reasonable assumption that the potential-energy surfaces of these states are similar. The correction scheme for vertical versus adiabatic transitions is the following. The adiabatic properties given below refer to 0 K values, i.e. they include the zero-point energies (ZPEs). The differences between vertical and adiabatic electron transfer were derived by calculating the energy of a certain species, e.g. $FeCl^-$, using the geometry obtained in the optimization of the same species having a different charge, e.g. $FeCl^+$ or FeCl. Thus, as an example, the energy difference of an $FeCl^-$ anion having the bond length of the geometry-optimized $FeCl^+$ cation ($r_{Fe–Cl}$ = 2.07 Å) and of the $FeCl^-$ minimum ($r_{Fe–Cl}$ = 2.30 Å) represents the energy difference between the vertical and adiabatic charge inversions $FeCl^+ \rightarrow FeCl^-$. This methodology implies a two-electron transfer in a single step for the transitions $FeCl_m^+ \rightarrow FeCl_m^-$ and $FeCl_m^- \rightarrow FeCl_m^+$ (m = 1–3). The vertical/adiabatic energy difference for a two-step, single-electron transfer scenario, e.g. $FeCl^+ \rightarrow FeCl \rightarrow FeCl^-$ was examined as well. However, because of the small geometry changes between the different charge states involved, the same results were obtained within the error of the method for both mechanistic schemes. Therefore, only the values for the above mentioned one-step, two-electron transfer are tabulated below. In the calculation of these energy differences, the ZPEs were not included.

Table 2
Ion intensities[a,b] observed in the CA, CR, and NR mass spectra[c] of B(1)/E(1) mass-selected $FeCl_m^n$ ions ($m = 1–4$; $n = -1, +1$)

	Spectrum	$FeCl_3$	$FeCl_2$	FeCl	Cl_2	Fe	Cl	Other species
$FeCl_3^-$	CA		100				10	
	$^-CR^+$	4	100	45	2	15	5	
	$^-NR^+$	6	40	100	1	35	8	
	$^-NIDD^+$[d]	1	−38	26	0	10	1	
$FeCl_4^-$[e]	CA	100	1				1	
	$^-CR^+$	60	90	100	4	15	8	
	$^-NR^+$	12	65	100	3	45	12	
	$^-NIDD^+$[d]	−17	−5	6	0	14	2	
$FeCl^+$	CA					100	1	$FeCl^{2+}$ (1)
	CS					100	2	$FeCl^{2+}$ (4)
	$^+NR^+$			100		40	3	
$FeCl_2^+$	CA			100		3		
	CS			100		4	<1	$FeCl_2^{2+}$ (<1)
	$^+NR^+$		95	100	1	25	3	
$FeCl_3^+$	CA		100	20		1		
	CS		100	15	<1	3	<1	$FeCl_3^{2+}$ (<1)
	$^+NR^+$	25	90	100	12	30	4	
$FeCl_4^+$[f]	CA	100	30	10				

[a] Given relative to the base peak = 100%.
[b] Contributions of ^{54}Fe and ^{37}Cl isotopes are neglected.
[c] Experimental conditions: CA, He, 80% transmission (T), $^-CR^+$, O_2, 80% T, $^-NR^+$, O_2/O_2, 80% T/80% T, $^+NR^+$, Xe/O_2, 80% T/80% T, CS, O_2, 80% T.
[d] $^-NIDD^+$ spectrum derived from the data of the $^-CR^+$ and $^-NR^+$ spectra given in the preceding lines. By definition, the sum of the NIDD intensities is zero; for details, see [15,16].
[e] Even at maximum sensitivity, no recovery signal due to $FeCl_4^+$ was observed.
[f] The intensity of $FeCl_4^+$ was too low for CS and $^+NR^+$ experiments.

4. Results and discussion

The data given in this section refer to $FeCl_m^n$ ions ($m = 1–4$; $n = -1, +1, +2$) generated by electron ionization (EI) of gaseous $FeCl_3$, and if not mentioned otherwise, the results obtained with chemical ionization (CI) of $Fe(CO)_5/Cl_2$ were identical within experimental error. This section is organized such that we first describe the experimental and theoretical results for the neutral and singly charged species, followed by the data for $FeCl_m^{2+}$ dications ($m = 1–3$). A comprehensive discussion of the experimental and theoretical results is given in the next section.

4.1. Dissociation behavior of $FeCl_m^n$ ions ($m = 1–4$; $n = -1, +1$)

As a consequence of the limited size of the system, none of the $FeCl_m^n$ species ($m = 1–3$; $n = -1, +1, +2$) underwent structure-specific unimolecular reactions. Thus, the corresponding metastable ion (MI) mass spectra were identical to the collisional activation (CA) mass spectra, except for much lower fragment ion intensities. In fact, rather than being due to metastable ions, the minor fragmentations observed in these experiments are likely to arise from collision-induced dissociation with residual background gases present in the mass spectrometer [22].

The CA spectra of the $FeCl_m^-$ anions ($m = 3, 4$) show simple fragmentation patterns in which losses of atomic chlorine prevail (Table 2). The fact that $FeCl_2^-$ is more intense than Cl^- in the CA spectrum of $FeCl_3^-$ although $EA(FeCl_2) = 0.99$ eV (Table 1) is lower than $EA(Cl) = 3.62$ eV [31] may be attributed to the mass discrimination in detecting Cl^- (35 u) versus $FeCl_2^-$ (126 u) [32] as well as the difference between the vertical and the adiabatic neutralization of $FeCl_2^-$ (see below). In turn, despite a moderate intensity of the $FeCl_2^-$, no significant CA mass spectrum was obtained, suggesting that electron detachment pre-

vails. This conclusion is in accord with EA($FeCl_2$) = 0.99 eV being much lower than the energy demands of the conceivably competing bond cleavages to afford FeCl + Cl^- (2.23 eV) and $FeCl^-$ + Cl (4.31 eV). Further, note that none of the spectra displays a significant signal due to formation of a Cl_2^- molecular anion although this species can be formed in keV collisions [15].

Sequential losses of atomic chlorine also prevail in the CA spectra of the $FeCl_m^+$ cations (m = 1–4). Besides some dication signals due to charge stripping (see below), there is in fact not much more to be extracted from the cation CA spectra, except the confirmation of the purity of the mass-selected ion beams in that no fragments other than those expected for $FeCl_m^+$ (m = 1–4) were observed.

Some information with respect to the fragmentation of the neutral iron chlorides $FeCl_m$ (m = 3, 4) can be obtained by quantitative analysis of the $^-CR^+$ and $^-NR^+$ spectra in terms of the recently introduced NIDD scheme [15,16]. The $^-CR^+$ and $^-NR^+$ spectra of $FeCl_3^-$ and $FeCl_4^-$ are dominated by intense signals due to $FeCl_m^+$ with m = 1, 2 for $FeCl_3^-$ and m = 1–3 for $FeCl_4^-$. The extensive degree of degradation in the spectra may be regarded as an indication for expulsions of molecular chlorine, rather than sequential losses of chlorine atoms. For example, the positive signal for $FeCl^+$ in the $^-NIDD^+$ spectrum of $FeCl_3^-$ suggests the fragmentation of the neutral species according to $FeCl_3 \rightarrow FeCl + Cl_2$. Occurrence of this reaction would, however, require that the complementary signal of Cl_2^+ formed upon reionization of neutral Cl_2 would increase in the $^-NR^+$ relative to the $^-CR^+$ spectrum, and thus appear on the positive scale of the $^-NIDD^+$ spectrum of $FeCl_3^-$ [15]. Experimentally, the Cl_2^+ intensities are low, and if any the signal belongs to the negative scales of the $^-NIDD^+$ spectra of $FeCl_3^-$ and $FeCl_4^-$. Instead, the positive $^-NIDD^+$ signals for Cl^+ are consistent with sequential Fe–Cl bond cleavages. The more extensive fragmentation in NR than in CR can be traced back to the fact that the former requires two high-energy collisions by definition, whereas the charge reversal of anions may well occur in a single collision [15,25]. In comparison, fragmentations are less pronounced in the $^+NR^+$ spectra of the $FeCl_m^+$ cations (m = 1–3), for which sizable recovery signals are observed. These differences are consistent with the smaller changes in geometry in the $^+NR^+$ sequence, i.e. $FeCl_m^+ \rightarrow FeCl_m \rightarrow FeCl_m^+$, compared to charge inversion, i.e. $FeCl_m^- \rightarrow FeCl_m^+$.

In essence, the fragmentation patterns of $FeCl_m^n$ (m = 3, 4 for n = −1, 0; m = 1–3 for n = +1) species confirm the intuitive conjecture that sequential reduction of the metal chlorides is more facile than loss of molecular chlorine. Some circumstantial evidence, which will be discussed further below, does indeed suggest that formation of Cl_2^+ is probably due to fragmentations of excited cation states.

Except for $FeCl_4^-$, all $FeCl_m^n$ (m = 1–3; n = −1, +1) species exhibit recovery signals in charge reversal as well as neutralization-reionization experiments. Specifically, $FeCl_m^-$ (m = 2, 3) and $FeCl_m^+$ (m = 1–3) yield reionized parent ions in $^-CR^+$, $^-NR^+$, $^+CR^-$, $^+NR^-$, and $^+NR^+$ experiments, respectively. Further, the $FeCl_m^+$ (m = 1–3) monocations give rise to the corresponding dication signals in charge stripping experiments (see below). These results are in accord with the expected, reasonably strong covalent bonds between iron and chlorine [2,8,9].

The mere presence of the recovery signals allows one to probe the redox properties of the iron chlorides in the gas phase by means of energy-resolved CR spectra of the recovery ions in which the associated energy differences (ΔE_{CR}) can be determined from the high-energy onsets of the recovery ions [21,23–25,28]. These experiments are quite sensitive because instead of full mass spectra, only a narrow region in the vicinity of the recovery signal is monitored. Compared to other spectroscopic techniques, however, the precision of the measured energies is poor, mostly because of the limited energy resolution of our mass spectrometer [33]. Experimentally, the following differences were determined: $\Delta E_{^-CR^+}(FeCl_2^-)$ = 11.9 ± 0.8 eV, $\Delta E_{^-CR^+}(FeCl_3^-)$ = 19.8 ± 1.1 eV, $\Delta E_{^+CR^-}(FeCl^+)$ = 14.7 ± 1.0 eV, $\Delta E_{^+CR^-}(FeCl_2^+)$ = 12.9 ± 0.8 eV, and $\Delta E_{^+CR^-}(FeCl_3^+)$ = 10.1 ± 0.9 eV; $FeCl_4^-$ did not yield a detectable recovery signal in $^-CR^+$. The relevance of these data with respect to the

Table 3
Computed adiabatic electron affinities (EA_a, eV), ionization energies (IE_a, eV) of $FeCl_m^n$ ($m = 1–3$; $n = -1, 0, +1$), and the respective bond dissociation energies (eV) $D_0(Fe–Cl^-)$, $D_0(Fe–Cl)$, and $D_0(Fe^+–Cl)$ of the iron chlorides as predicted by B3LYP/6-311+G* calculations.[a,b] In addition, some calculated properties of the atomic fragments along with experimental values (in brackets)[c] are given

	EA	IE	$D_0(Fe–Cl^-)$	$D_0(Fe–Cl)$	$D_0(Fe^+–Cl)$
FeCl	1.91	7.91	1.63	3.45	3.46
$FeCl_2$	1.09	10.29	1.94	4.58	2.19
$FeCl_3$	4.31	10.93	2.68	2.09	1.44
Fe		7.99 (7.89)			
Fe^+		16.51 (16.18)			
Cl	3.72 (3.62)	13.08 (12.97)			
Cl_2		11.59 (11.48)[d]			

[a] Calculated electronic states and optimized Fe–Cl bond lengths r: $r(FeCl^-, {}^5\Delta) = 2.30$ Å, $r(FeCl, {}^6\Delta) = 2.21$ Å, $r(FeCl^+, {}^5\Delta) = 2.07$ Å, $r(FeCl_2^-, {}^6A_1) = 2.32$ Å and $\alpha = 110°$, $r(FeCl_2, {}^5\Delta) = 2.15$ Å and $\alpha = 180°$, $r(FeCl_2^+, {}^6A_1) = 2.08$ Å and $\alpha = 140°$, $r(FeCl_3^-, {}^5A') = 2.26$ Å, $r(FeCl_3, {}^6A') = 2.15$ Å, $r(FeCl_3^+, {}^5A') = 2.08$ Å; all iron trichlorides were found to have D_{3h} symmetry.

[b] All data refer to the Fe^+ (^6D) ground state. Note that B3LYP/6-311+G* wrongly predicts Fe^+ (^4F) to be 0.22 eV more stable than Fe^+ (^6D) (see also [8–10]); the experimentally determined state splitting is 0.23 eV in favor of Fe^+ (^6D).

[c] Taken from [31].

[d] B3LYP significantly underestimates $D_0(Cl–Cl)$, predicting a value of only 46.9 kcal/mol compared to the experimental value (57.2 kcal/mol [31]).

associated vertical electron transfers involved is discussed further below.

4.2. B3LYP calculated thermochemistry of $FeCl_m^n$ ($m = 1–3$, $n = -1, 0, +1$)

In comparison with the data evaluated by Bach et al. [8] (Table 1), our B3LYP/6-311+G* approach generally performs quite well for the iron chlorides (Table 3). Similar conclusions were drawn by Bauschlicher [9] and Glukhovtsev et al. [10] in their recent computational studies of iron halides. In fact, the reasonable accuracy of the empirical B3LYP hybrid functional in conjunction with moderate computational costs is a major factor for the extensive application of this method.

Upon closer inspection, the deviations of the B3LYP energetics from the data given in Table 1 increase with the formal oxidation state of iron, i.e. whereas the bond energies for anionic, neutral, and cationic FeCl are reproduced reasonably well with B3LYP, the Fe–Cl bond strengths in cationic $FeCl_2^+$ as well as neutral $FeCl_3$ are underestimated by 0.33 and 0.46 eV, respectively. Although this inaccuracy seems acceptable, some evidence discussed further below indicates that the B3LYP approach may exhibit some systematic errors as to the absolute energetics of electron transfer that also involves a change of the formal oxidation state. Notwithstanding, we are confident that B3LYP treats the species of interest reasonably well in the vicinity of the respective minima. For example, B3LYP has been shown to provide accurate geometries for neutral and charged iron compounds [8–10,30]. Thus, the B3LYP/6-311+G* level of theory is assumed to yield good predictions for the differences between vertical and adiabatic electron transfer for the systems of interest (Table 4), even though the absolute values may be less reliable (see below).

Not unexpected for transition metal halides, the geometries of $FeCl_m^n$ ($m = 1–3$; $n = -1$, $+1$) change smoothly upon sequential oxidation or reduction. The Fe–Cl bond lengths slightly decrease from the anionic to the cationic species, and most changes are not all that dramatic. For example, the computed stabilities of $FeCl^-$ relative to FeCl are -1.90 eV for the optimized anion ($r_{Fe–Cl} = 2.30$ Å), -1.87 eV for the anion having the bond length of neutral FeCl ($r_{Fe–Cl} = 2.21$ Å), and -1.64 eV for the anion having the bond length of $FeCl^+$ ($r_{Fe–Cl} = 2.07$ Å). Similarly, the vertical ionizations of the neutral and anion

Table 4
Calculated B3LYP/6-311+G* energies (in eV) for $FeCl_m^n$ species ($m = 1–3$; $n = -1, 0, +1$) having the optimized geometries of the anionic, neutral, and cationic minima, respectively[a,b,c]

Species	Geometry	FeCl	$FeCl_2$	$FeCl_3$
Cation	Cation	*7.90*	*10.29*	*10.93*
	Neutral	8.05	10.40	11.16
	Anion	8.26	11.10	11.57
Neutral	Cation	0.13	0.31	0.30
	Neutral	*0.00*	*0.00*	*0.00*
	Anion	0.05	0.91	0.23
Anion	Cation	−1.64	−0.27	−3.50
	Neutral	−1.87	0.20	−3.75
	Anion	*−1.90*	*−1.08*	*−4.30*

[a] All energies are given relative to the corresponding neutral iron chloride.
[b] The adiabatic properties (IE_a and $-EA_a$) are given in italics.
[c] Zero-point energies are not included.

structures to $FeCl^+$ and $FeCl_3^+$ cations result in energy differences of no more than 0.6 eV compared to the adiabatic processes. The largest differences between vertical and adiabatic transitions are found for iron dichloride. This effect can be attributed to the fact that neutral $FeCl_2$ is linear, whereas $FeCl_2^-$ and $FeCl_2^+$ have bent structures [8,34]. For the geometry-optimized structure of $FeCl_2^-$ ($r_{Fe–Cl} = 2.32$ Å, $\alpha = 110°$), B3LYP/6-311 + G* predicts an adiabatic $EA_a(FeCl_2)$ of 1.08 eV that compares reasonably well with $EA_a(FeCl_2) = 0.99$ eV [8]. However, the vertical electron affinity of $FeCl_2$ having the structure obtained in the geometry optimization of the cationic species ($r_{Fe–Cl} = 2.08$ Å, $\alpha = 140°$) is only 0.27 eV. The vertical electron affinity of the linear, neutral $FeCl_2$ molecule ($r_{Fe–Cl} = 2.15$ Å, $\alpha = 180°$) is even predicted to be negative, $EA_v(FeCl_2) = -0.20$ eV. In this particular case, bending seems therefore to be more important for the stability of $FeCl_2^-$ anion than the differences in $r_{Fe–Cl}$.

4.3. $FeCl_m^{2+}$ ($m = 1–3$) dications

The first systematic charge-stripping studies of transition-metal halides are credited to Lebrilla and co-workers [35–37]. In the present system, we find that the $FeCl_m^+$ monocations ($m = 1–3$) can be oxidized to the corresponding dications upon charge stripping (CS) with molecular oxygen in keV collisions (Table 2). Relative to the base peaks of the CS spectra (Table 2), the intensities of the charge-stripping signals are 4% for $FeCl^{2+}$, 0.2% for $FeCl_2^{2+}$, and about 0.05% for $FeCl_3^{2+}$. Thus, intensities of the $FeCl_m^{2+}$ dication signals relative to the other, singly charged fragments decrease with increasing m. This trend can be regarded as a consequence of the increasing manifold of low-lying fragmentation channels for $FeCl_2^+$ and $FeCl_3^+$ compared to diatomic $FeCl^+$ in conjunction with the corresponding dication stabilities (see below). Energy-resolved charge-stripping experiments yield $Q_{min}(FeCl^+) = 15.9 \pm 0.4$ eV, $Q_{min}(FeCl_2^+) = 17.6 \pm 0.7$ eV, and $Q_{min}(FeCl_3^+) = 16.0 \pm 0.4$ eV. Within the experimental uncertainty, EI of gaseous $FeCl_3$ and CI of $Fe(CO)_5/Cl_2$ gave identical Q_{min} values for $FeCl^+$ and $FeCl_3^+$. Charge stripping of $FeCl_2^+$, however, deserves some more detailed discussion. At first, the experimental error of Q_{min} ($FeCl_2^+$) is significantly larger than those of $Q_{min}(FeCl^+)$ and $Q_{min}(FeCl_3^+)$, although the ions were examined under essentially identical conditions. Second, whereas EI of gaseous $FeCl_3$ yields $Q_{min}(FeCl_2^+) = 17.6 \pm 0.7$ eV, a drastic decrease to $Q_{min}(FeCl_2^+) = 15.2 \pm 0.5$ eV occurs when the monocation precursurs are generated by CI of $Fe(CO)_5/Cl_2$. Both findings suggest contributions of isomeric structures and/or excited states present in the $FeCl_2^+$ precursor ion beam; this aspect is discussed in more detail further below.

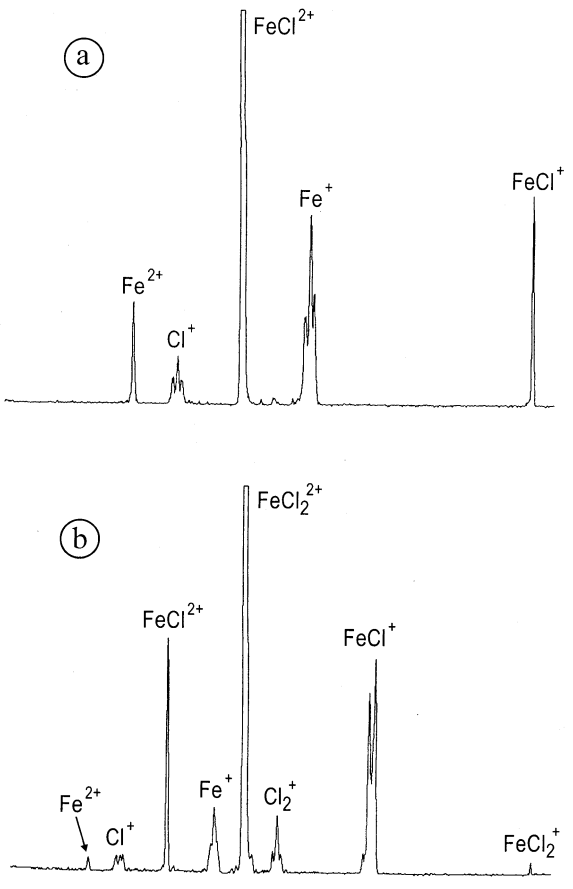

Fig. 1. (a) Charge-exchange spectrum of B(1)/E(1) mass-selected $FeCl^{2+}$ dication (helium, 80% T). Note that the $FeCl^{2+}$ precursor is off scale; the gain factor is 500. The Fe^+ and Cl^+ signals show typical peak shapes due to overlap of charge exchange and Coulomb explosion. (b) Charge-exchange spectrum of B(1)/E(1) mass-selected $FeCl_2^{2+}$ dication (helium, 60% T). Note that the $FeCl_2^{2+}$ precursor is off scale; the gain factor is 300. The $FeCl^+$, Cl_2^+, Fe^+, and Cl^+ signals show typical peak shapes due to overlap of charge exchange and Coulomb explosion.

$FeCl_m^{2+}$ dications (m = 1–3) can also be generated directly by EI of gaseous $FeCl_3$. The intensities of $FeCl^{2+}$ and $FeCl_2^{2+}$ were sufficient to probe the dications in charge-exchange (CE) experiments using helium as a collision gas. The CE spectrum of $FeCl^{2+}$ [Fig. 1(a)] displays signals due to monocations of $FeCl^+$, Fe^+, and Cl^+ as well as the Fe^{2+} dication due to homolytic bond cleavage of the dication. The Fe^+ and Cl^+ signals are composite, showing characteristic features due to Coulomb explosion of $FeCl^{2+}$ into $Fe^+ + Cl^+$. Thus, the central components of the peaks are due to charge exchange followed by fragmentation of the $FeCl^+$ monocation, whereas the high- and low-mass components can be assigned to dished-topped peaks arising from charge separation of the $FeCl^{2+}$ dication. Similarly, the CE spectrum of $FeCl_2^{2+}$ [Fig. 1(b)] shows composite peaks that can be attributed to charge exchange as well as the charge separations into $FeCl^+ + Cl^+$ and $Fe^+ + Cl_2^+$, respectively. In addition, some charge exchange to afford $FeCl_2^+$ monocation is observed as well as homolytic bond cleavages of the dication resulting in formation of $FeCl^{2+}$ and Fe^{2+}. In the corresponding CE spectra with oxygen as collision gas (not shown), formation of monocations due to charge exchange prevails. The differences in CE with oxygen and helium as the collision gases can be explained by considering that $IE(O_2)$ = 12.07 eV [31] is much lower than $IE(FeCl_m^+) \approx 15$–18 eV (see above), such that despite a Coulombic barrier, electron transfer from the target to the dication is favorable for oxygen, whereas charge exchange is quite endothermic with helium (IE(He) = 24.48 eV [31]) as a collision partner.

The B3LYP/6-311+G* calculations predict very minor geometry changes going from the $FeCl_m^+$ monoto the $FeCl_m^{2+}$ dications (m = 1–3), i.e. $r_{Fe–Cl}$ = 2.07 Å in $FeCl^+$ ($^5\Delta$) versus 2.08 Å in $FeCl^{2+}$ ($^6\Sigma$), $r_{Fe–Cl}$ = 2.08 Å in $FeCl_2^+$ ($^6A_1$) versus 2.09 Å in $FeCl_2^{2+}$ ($^5B_2$), $r_{Fe–Cl}$ = 2.08 Å in $FeCl_3^+$ ($^5A'$) versus 2.09 Å in $FeCl_3^{2+}$ ($^6A''$). Therefore, we consider that the vertical and adiabatic ionization energies of the monocations are more or less identical and regard the measured Q_{min} values as good approximations for the adiabatic IEs of the iron halide cations. Compared to the results for the singly charged and neutral iron chlorides, the agreement between the experimental and calculated energetics is poor for $FeCl^{2+}$ and $FeCl_3^{2+}$. Thus, the computed IEs are more than 1 eV larger than the measured Q_{min} values for these ions, whereas the data agree reasonably well for $FeCl_2^{2+}$ (see Table 5). We shall return to this discrepancy further below.

A further, interesting aspect concerns the $FeCl_2^{2+}$ dication. In addition to the bent iron dichloride dication $FeCl_2^{2+}$ ($^5B_2$) with $r_{Fe–Cl}$ = 2.09 Å and α = 99°,

Table 5
Measured Q_{min} values (eV), calculated[a] ionization energies (IE, eV) of $FeCl_m^+$ monocations (m = 1–3)

	Q_{min}[b]	IE[c]
$FeCl^+$	15.9 ± 0.4	17.19
$FeCl_2^+$	17.6 ± 0.7[d]	17.42
	15.2 ± 0.5[e]	13.72[f]
$FeCl_3^+$	16.0 ± 0.4	17.04

[a] B3LYP/6-311+G*

[b] The error bars include the experimental uncertainty (one standard deviation) of several independent measurements using charge stripping of ionized toluene as a reference.

[c] Differences between vertical and adiabatic IE were neglected, because the geometries of mono- and dications match each other within <0.02 Å.

[d] EI of $FeCl_3$.

[e] CI of $Fe(CO)_5/Cl_2$.

[f] Here, the computed value refers to the adiabatic transition $Fe(Cl_2)^+ \rightarrow Fe(Cl_2)^{2+}$; the respective vertical ionization of $Fe(Cl_2)^+$ is expected to be higher in energy (see text).

the B3LYP calculations predict the existence of a second minimum with $r_{Fe–Cl}$ = 2.40 Å, α = 51°, and a $r_{Cl–Cl}$ distance of only 2.09 Å. This isomer is best described as molecular chlorine complexed to Fe^{2+} dication, i.e. $Fe(Cl_2)^{2+}$ ($^5A_1$). Moreover, the B3LYP calculations predict $Fe(Cl_2)^{2+}$ ($^5A_1$) to be 0.58 eV lower in energy than $FeCl_2^{2+}$ ($^5B_2$). Accordingly, we also searched for an isomeric species for the monocation and were able to locate a $Fe(Cl_2)^+$ ($^6A_1$) species with $r_{Fe–Cl}$ = 2.82 Å and $r_{Cl–Cl}$ = 2.06 Å on the sextet surface that is calculated to be 3.1 eV higher in energy than the $FeCl_2^+$ ($^6A_1$) ground state. Thus, the adiabatic IE of this isomer is predicted as IE($Fe(Cl_2)^+$) = 13.7 eV. Considering the significant difference in $r_{Fe–Cl}$ between $Fe(Cl_2)^+$ and $Fe(Cl_2)^{2+}$, the experimentally measured Q_{min} value of 15.2 ± 0.5 eV is in qualitative agreement with the theoretical findings.

Finally, we carefully examined the source spectra for the possible formation of long-lived $FeCl_m^{3+}$ trications (m = 1–3) [19,20] as well as $FeCl_m^{2-}$ dianions (m = 3, 4) [38] and further tried to generate $FeCl_m^{3+}$ by charge stripping of the corresponding dications (m = 1, 2). However, in none of these studies did we find any indications for the formation of these multiply charged ions.

5. Redox properties of $FeCl_m^n$ (m = 1–3, n = −1, 0, +1, +2)

The experimentally determined redox properties of the iron chlorides agree reasonably well with the literature thermochemistry (Table 1), if the differences between vertical and adiabatic electron transfer are taken into account.

The experimental value $\Delta E^-_{CR^+}(FeCl_2^-)$ = 11.9 ± 0.8 eV is somewhat larger than the sum of the adiabatic EA_a and IE_a of $FeCl_2$ (11.1 eV). Nevertheless, the difference agrees nicely with the calculated energy difference of 0.81 eV between ground state $FeCl_2^+$ and the cation having the geometry of the anionic species ($r_{Fe–Cl}$ = 2.32 Å, α = 110°). In contrast, the experimental $\Delta E^-_{CR^+}(FeCl_3^-)$ = 19.8 ± 1.1 eV is far beyond the sum of EA_a and IE_a (~14.8 eV), suggesting that charge inversion of $FeCl_3^-$ leads to the formation of $FeCl_3^+$ in a high-lying electronically excited state. Apparently, generation of long-lived, ground state $FeCl_3^+$ is disfavored by the energy disposal in the keV collision in conjunction with the low Cl_2Fe^+–Cl bond strength (1.44 eV, Table 3).

For analyzing the charge inversion of cations, the net energy balances have to be considered, i.e. $\Delta E^+_{CR^-}$ = 2 · IE(Xe) − $RE_v(FeCl_m^+)$ − $EA_v(FeCl_m)$, where RE_v is the vertical recombination energy of the cation and EA_v is the vertical electron affinity of the neutral. Note that the more likely mechanism, e.g. stepwise single-electron transfer, is assumed in the above equation (see Sec. 2). With IE(Xe) = 12.13 eV [31], the measured set of data $\Delta E^+_{CR^-}(FeCl^+)$ = 14.7 ± 1.0 eV, $\Delta E^+_{CR^-}(FeCl_2^+)$ = 12.9 ± 0.8 eV, and $\Delta E^+_{CR^-}(FeCl_3^+)$ = 10.1 ± 0.9 eV translates into $RE_v(FeCl^+)$ + $EA_v(FeCl)$ = 9.6 ± 1.0 eV, $RE_v(FeCl_2^+)$ + $EA_v(FeCl_2)$ = 11.4 ± 0.8 eV, and $RE_v(FeCl_3^+)$ + $EA_v(FeCl_3)$ = 14.2 ± 0.9 eV. These sums agree reasonably well with literature data. For the process $FeCl^+ \rightarrow FeCl^-$ the sum of IE_a and EA_a amounts to 9.43 eV (Table 1), and the energy difference due to vertical charge inversion of the cation is only 0.26 eV (Table 4). For $FeCl_2$, the experimental figure is also consistent with IE_a + EA_a = 11.1 eV, although a somewhat lower value would have been expected, if only the vertical

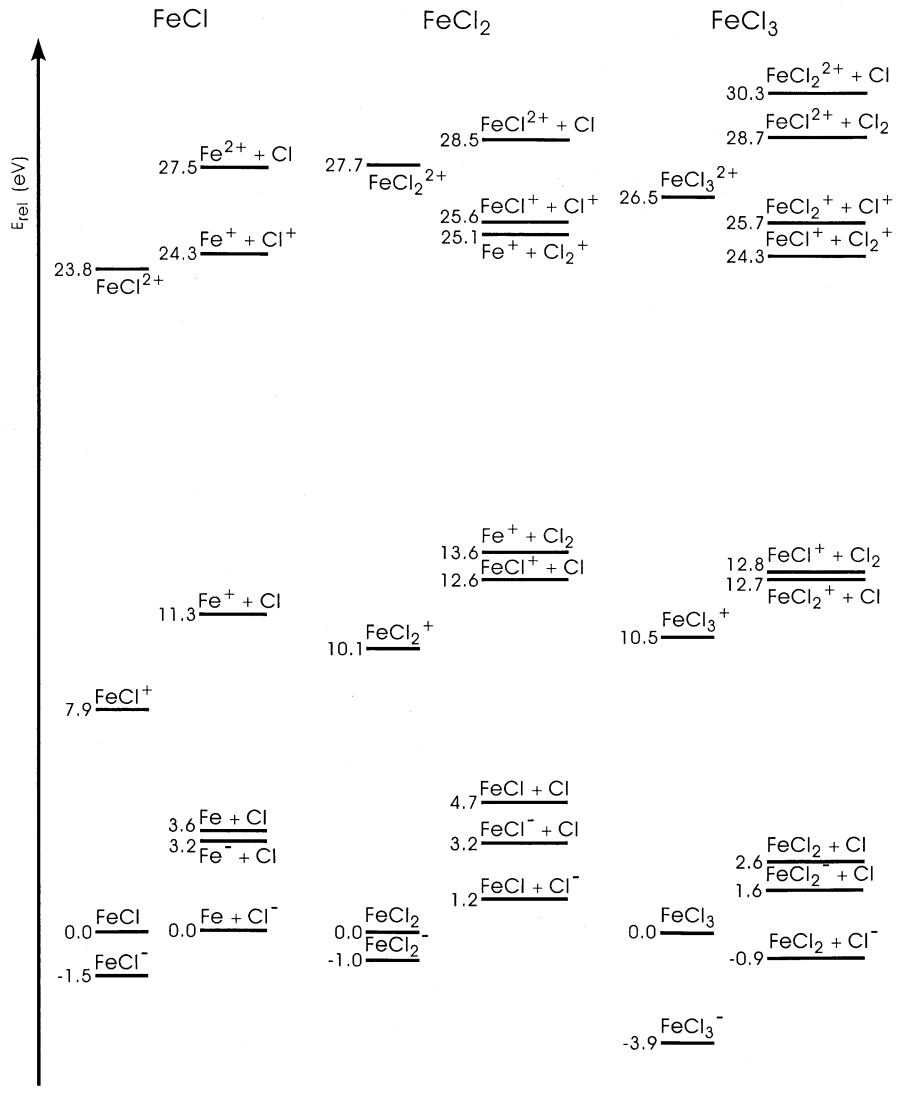

Fig. 2. Redox properties and thermochemical stabilities (in eV) of $FeCl_m^n$ (m = 1–3; n = −1, 0, +1, +2) species and relevant fragmentation channels relative to the respective neutral iron chlorides as obtained from experiments.

transition $FeCl_2^+ \rightarrow FeCl_2^-$ occurs. Finally, the experimental value for $FeCl_3^+$ agrees with IE_a + EA_a = 14.8 eV, and the additional energy demand of 0.80 eV associated with the vertical transition $FeCl_3^+ \rightarrow FeCl_3^-$. The differences between vertical and adiabatic electron transfer appear to be less important in the charge inversion of cations [28]. This finding is indeed plausible because the high-energy onsets of the $^+CR^-$ signals on the kinetic energy scale are due to occurrence of sequential electron transfer from the target to the projectile in two separate collisions rather than double electron transfer in a single collision event [15,23] provided that the transient neutral species have lifetimes in (or beyond) the microsecond regime [25]. This analysis of the redox properties (Fig. 2) used one particular value that is not given in [8], i.e. the ionization energy of $FeCl_3$. For the time being, we rely on

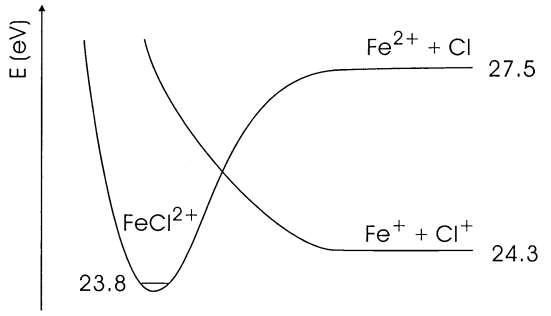

Fig. 3. Schematic potential-energy curves for $FeCl^{2+}$ dication. The energies (in eV) are derived from the experimental data and are given relative to neutral FeCl.

$IE(FeCl_3)$ = 10.93 eV as predicted by the B3LYP/6-311+G* calculations, although this value is likely to be slightly too large (see below).

Using thermochemical cycles with known properties of the fragments, the Q_{min} values allow one to assess the dication stabilities with respect to the corresponding dissociation asymptotes [37]. According to the measured $Q_{min}(FeCl^+)$ = 15.9 ± 0.4 eV, $FeCl^{2+}$ adds to the series of thermochemically stable, diatomic dications, of which most belong to the metal halide series [19,20,39]. Thus, $D(Fe^{2+}–Cl)$ = 3.7 ± 0.5 eV is significant and Coulomb explosion to $Fe^+ + Cl^+$ is calculated to be endothermic by 0.5 ± 0.5 eV (Fig. 3). Considering that charge separation is hindered by a Coulombic barrier, whereas simple bond homolysis to afford Fe^{2+} can be assumed to have no barrier in excess of endothermicity, the sizable amount of the Fe^{2+} fragment in CE spectrum of $FeCl^{2+}$ [Fig. 1(a)] finds a rationale. These results imply that the Fe–Cl bond strength is slightly larger in the dication than in the monocation. This conclusion is qualitatively consistent with the removal of a formally nonbonding electron in the transition $FeCl^+$ ($^5\Delta$) → $FeCl^{2+}$ ($^6\Sigma$).

The $FeCl_2^{2+}$ and $FeCl_3^{2+}$ dications are predicted to be metastable with respect to Coulomb explosion (Fig. 2). Interestingly, the CE spectrum of $FeCl_2^{2+}$ [Fig. 1(b)] does not only show charge separation into $FeCl^+ + Cl^+$ but also peaks due to $Fe^+ + Cl_2^+$. Thus, the dication surface allows for formation of the dichloride $FeCl_2^{2+}$ species as well as the $Fe(Cl_2)^{2+}$ isomer in which molecular chlorine is complexed to Fe^{2+}. In fact, the B3LYP calculations predict that $Fe(Cl_2)^{2+}$ is more stable than $FeCl_2^{2+}$. This energetic situation of the dications as well as the associated fragmentation channels are shown in Fig. 4.

The existence of two structural isomers of the dication also explains the significant dependence of the Q_{min} values from mode of ion generation. Whereas EI of gaseous $FeCl_3$ is assumed to yield $FeCl_2^+$ cation exclusively, CI of $Fe(CO)_5/Cl_2$ may also lead to the formation of the isomeric $Fe(Cl_2)^+$ monocation via ligand exchange, e.g. $Fe(CO)^+ + Cl_2 \rightarrow Fe(Cl_2)^+ + CO$. Even if this isomer is formed in only very small quantities, its propensity to undergo charge

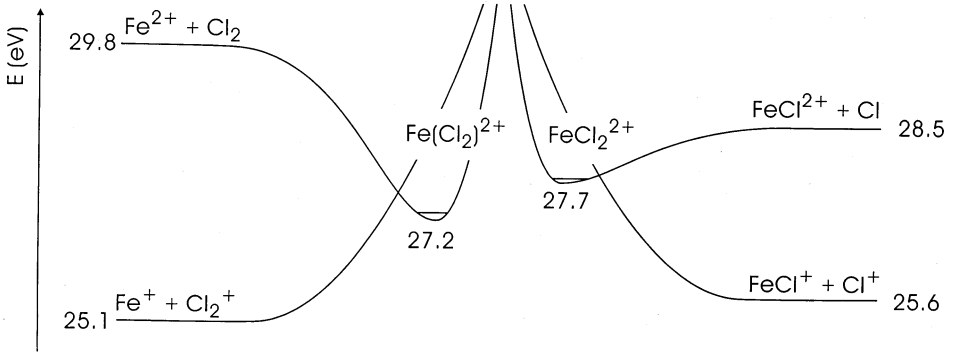

Fig. 4. Schematic potential-energy curves (energies in eV) for the $Fe(Cl_2)^{2+}$ and $FeCl_2^{2+}$ dications. The area in which the curves intersect is arbitrarily chosen and actually unknown. The energies (in eV) are derived from the experimental data and are given relative to neutral $FeCl_2$; an exception is $Fe(Cl_2)^{2+}$ which was located according to the calculated stability difference between $Fe(Cl_2)^{2+}$ and $FeCl_2^{2+}$ (see text).

stripping is much larger, because the energy required for ionization to the dication is significantly lower than for the iron dichloride. Thus, the B3LYP calculations predict $IE_a(Fe(Cl_2)^+) = 13.7$ eV and $IE_a(FeCl_2^+) = 17.4$ eV. Note that the stabilities of $Fe(Cl_2)^{+/2+}$ relative to $FeCl_2^{+/2+}$ may be underestimated by theory, because bonding of molecular chlorine is not properly described with B3LYP/6-311+G* (see footnote to Table 3).

Finally, the significant deviation between the experimental and theoretical data for $FeCl^{2+}$ and $FeCl_3^{2+}$ should be discussed (Table 5). The measured Q_{min} values are more than 1 eV lower than the calculated figures. In fact, the calculations predict that $FeCl^{2+}$ dication is not thermochemically stable as implied by $Q_{min}(FeCl^+)$, but metastable with respect to the Coulomb explosion into Fe^+ and Cl^+. As noted above, Franck–Condon effects cannot account for these discrepancies, because the geometries of the mono- and dications are reasonably close to each other. Moreover, even if there were significant differences between the vertical and adiabatic ionization energies, these would result in Q_{min} values that are larger than the adiabatic IEs. The opposite trend is observed, however. The deviation between theory and experiment is clearly beyond the previously reported uncertainty of the B3LYP approach in calculating thermochemical properties of iron compounds [8–10] and demands more detailed consideration.

As far as the experiments are concerned, Q_{min} values lower than IE_a can only occur if a considerable fraction of the precursor monocations is electronically excited. Electronic excitation is indeed conceivable in ion generation using conventional ion sources. Nevertheless, the observation that the Q_{min} values of $FeCl^+$ and $FeCl_3^+$ were identical within experimental error under EI and CI conditions disfavors this option [40]. Note, however, that a secure thermalization of the precursor ions cannot be assumed in our experiments, and other approaches are required for a more definitive elaboration.

Notwithstanding these objections, some trends in the computational results indicate that the B3LYP approach may systematically underestimate dication stabilities. In fact, this level of theory seems to be generally inadequate for a quantitative description of redox properties. To illustrate this criticism, let us consider Tables 1 and 3 in some more detail. As stated above, on average B3LYP seems to perform quite well compared to the data given in Table 1, however, the deviations are not statistically spread, but deviate systematically. As previously outlined by Bauschlicher [9], this behavior can be attributed to the imperfect treatment of electron correlation with B3LYP resulting in a systematic overestimation of stabilities with an increasing number of electrons in a given system. This pitfall results in an artificial stabilization of low oxidation states, and the trend is indeed clearly shown by comparison of the data given in Tables 1 and 3. The computed EAs are up to 0.4 eV larger with B3LYP, i.e. the anions are too stable. On the other hand, B3LYP slightly overestimates the IEs, i.e. the cations' stabilities are too low. The same conclusion can be drawn from the comparison of the data for the atomic fragments in the lower part of Table 3. With B3LYP/6-311+G*, the EA of chlorine is overestimated by 0.1 eV as compared to the experimental figure, and along this trend the ionization energies of Fe, Cl, and Cl_2 are about 0.1 eV too large. Accordingly, it is also not surprising that $IE(Fe^+)$ is overestimated by 0.33 eV with B3LYP, and that the computed energy demand for the double ionization $Fe \rightarrow Fe^{2+}$ is 0.42 eV above experiment. The present data base is much too limited to assess the generality of this trend, an effort that would be far beyond the scope of the present study. It appears, however, that B3LYP and related density functional methods show systematic deficiencies in predicting IEs and EAs, not only for transition metals [9], but also—less pronounced—for main group elements [41]. Hopefully, this special issue on the chemistry and physics of multiply charged ions will shed further light on the performance of B3LYP with respect to dication stabilities.

Finally, let us briefly address the formation of Cl_2^+ as a prominent fragment (>10%) in the $^+NR^+$ spectrum of $FeCl_3^+$ (Table 2) and the CE spectrum of $FeCl_2^{2+}$ [Fig. 1(b)]. In both cases, we believe that this particular fragment is due to reactions of electroni-

cally excited monocation states formed in the electron-transfer processes involved. Let us begin by analyzing the situation for $FeCl_3^+$. If the Cl_2^+ fragment in the $^+NR^+$ spectrum of $FeCl_3^+$ was due to collisional activation of $FeCl_3^+$ ground state after reionization, the same fragment would be expected upon collisional activation of $FeCl_3^+$. In the corresponding CA and CS spectra of $FeCl_3^+$, however, the Cl_2^+ signals are negligible. Further, formation of molecular chlorine by dissociation of neutral $FeCl_3$ is disfavored by the analysis of the $^-NIDD^+$ spectrum of $FeCl_3^-$ (see above). Generation of electronically excited $FeCl_3^+$ is supported by the large value of $\Delta E_{^-CR^+} = 19.8 \pm 1.1$ eV determined for charge inversion of $FeCl_3^-$, which is ~5 eV above the energy demand of the corresponding adiabatic transition $FeCl_3^- \rightarrow FeCl_3^+$. An even more direct hint for the formation of excited monocation states giving rise to the Cl_2^+ fragment is the pronounced central component of the Cl_2^+ signal in the CE spectrum of $FeCl_2^{2+}$ [Fig. 1(b)]. Because this component of the peak is not broadened due to Coulomb explosion, it must originate from a monocation species. The latter is unlikely to correspond to the $FeCl_2^+$ ground state, because otherwise the Cl_2^+ fragment is expected to appear in the CA and CS spectra of $FeCl_2^+$ as well, which is not the case. Moreover, the similar magnitudes of the central components of the Fe^+ and Cl_2^+ signals in Fig. 1(b) conflict with thermochemistry, which implies a large preference for formation of Fe^+ instead of Cl_2^+, i.e. IE(Fe) = 7.89 eV versus IE(Cl_2) = 11.48 eV. Similar arguments apply if the ground state of the $Fe(Cl_2)^+$ isomer is considered. Therefore, we remain with the suggestion that an electronically excited monocation is inter alia formed upon charge exchange of $FeCl_2^{2+}$ dication with helium.

6. Conclusions

Electron transfer from or to iron chlorides can be probed using tandem mass spectrometry, thereby revealing the stabilities and possible dissociation processes ranging from the monoanions to the dications. In addition, energy-resolved experiments allow for an evaluation of gas-phase thermochemistry, although the precision is limited. Energy-resolved charge stripping remains, however, one of the few fundamental methods to determine dication energetics [18]; particular significance is achieved if the differences between vertical and adiabatic ionization are taken into account. For $FeCl_2^n$ ($n = +1, +2$), charge stripping even provides firm evidence for the existence of isomeric $Fe(Cl_2)^n$ species, at both the mono- and dication surfaces.

Nevertheless, there remain some uncertainties with respect to the conversion of measured Q_{min} values into adiabatic ionization energies. In particular, ion production in a conventional ion source cannot safely exclude the formation of electronically excited monocations, which would lead to Q_{min} values lower than the adiabatic ionization energies of the monocations. On the other hand, our results cast some doubt on the accuracy of the currently popular B3LYP approach for describing properly dicationic species. With respect to the sizable discrepancies between the theoretically predicted and experimentally measured ionization energies of $FeCl_m^+$, further experimental and theoretical efforts are indicated. Considering the volatility of $FeCl_3$ as well as the minor geometry differences between the mono- and dications, photoionization studies of $FeCl_3$ could be particularly helpful and could possibly provide additional anchor points for the accurate calibration of the energy scales employed in charge-stripping experiments.

Acknowledgements

Continuous financial support by the Deutsche Forschungsgemeinschaft, the Fonds der Chemischen Industrie, the Volkswagen-Stiftung, and the Gesellschaft von Freunden der Technischen Universität Berlin is gratefully acknowledged. We thank Dr. Ilona Kretzschmar for helpful discussions, and we are grateful to the Konrad-Zuse-Zentrum Berlin for the generous allocation of computer time.

References

[1] M.L. Mandich, M.L. Steigerwald, W.D. Reents Jr., J. Am. Chem. Soc. 108 (1986) 6197.
[2] A.E. Alvarado-Swaisgood, J.F. Harrison, J. Phys. Chem. 92 (1988) 5896.
[3] E.R. Fisher, R.H. Schultz, P.B. Armentrout, J. Phys. Chem. 93 (1989) 7382.
[4] R. Bakthiar, J.J. Drader, D.B. Jacobson, Org. Mass Spectrom. 28 (1993) 797.
[5] D. Schröder, J. Hrušák, H. Schwarz, Ber. Bunsenges. Phys. Chem. 97 (1993) 1085.
[6] M. Tanimoto, S. Saito, T. Okabayashi, Chem. Phys. Lett. 242 (1995) 153.
[7] D.L. Hildenbrand, J. Chem. Phys. 103 (1995) 2634.
[8] R.D. Bach, D.S. Shobe, H.B. Schlegel, C.J. Nagel, J. Phys. Chem. 100 (1996) 8770.
[9] C.W. Bauschlicher, Chem. Phys. 211 (1996) 163.
[10] M.N. Glukhovtsev, R.D. Bach, C.J. Nagel, J. Phys. Chem. A 101 (1997) 316.
[11] S.G. Wang, W.H.E. Schwarz, J. Chem. Phys. 109 (1998) 7252.
[12] C.A. Schalley, D. Schröder, H. Schwarz, Int. J. Mass Spectrom. Ion Processes 153 (1996) 173.
[13] M.M. Bursey, Mass Spectrom. Rev. 9 (1990) 555.
[14] N. Goldberg, H. Schwarz, Acc. Chem. Res. 27 (1994) 347.
[15] C.A. Schalley, G. Hornung, D. Schröder, H. Schwarz, Int. J. Mass Spectrom. 172/173 (1998) 181.
[16] C.A. Schalley, G. Hornung, D. Schröder, H. Schwarz, Chem. Soc. Rev. 27 (1998) 91.
[17] T. Ast, Adv. Mass Spectrom. A 8 (1980) 555.
[18] K. Vékey, Mass Spectrom. Rev. 14 (1995) 195, and references therein.
[19] D. Schröder, J.N. Harvey, H. Schwarz, J. Phys. Chem. A 21 (1998) 3639.
[20] D. Schröder, M. Diefenbach, T.M. Klapötke, H. Schwarz, Angew. Chem. Int. Ed. Engl. 38 (1999) 137.
[21] J.N. Harvey, C. Heinemann, A. Fiedler, D. Schröder, H. Schwarz, Chem. Eur. J. 2 (1996) 1230.
[22] D. Schröder, H. Schwarz, Int. J. Mass Spectrom. Ion Processes 146/147 (1995) 183.
[23] D. Schröder, J.N. Harvey, M. Aschi, H. Schwarz, J. Chem. Phys. 108 (1998) 8446.
[24] D. Schröder, C.A. Schalley, N. Goldberg, J. Hrušák, H. Schwarz, Chem. Eur. J. 2 (1996) 1235.
[25] D. Schröder, C. Heinemann, H. Schwarz, J.N. Harvey, S. Dua, S.J. Blanskby, J.H. Bowie, Chem. Eur. J. 4 (1998) 2550.
[26] N. Jeffreys, I.W. Griffiths, D.E. Parry, F.M. Harris, Int. J. Mass Spectrom. Ion Processes 164 (1997) 133, and references therein.
[27] K. Lammertsma, P.v.R. Schleyer, H. Schwarz, Angew. Chem. Int. Ed. Engl. 28 (1989) 1321.
[28] J.N. Harvey, D. Schröder, H. Schwarz, Bull. Soc. Chim. Belg. 106 (1997) 447.
[29] GAUSSIAN94, Revision B.3, M.J. Frisch, G.W. Trucks, H.B. Schlegel, P.M.W. Gill, B.G. Johnson, M.A. Robb, J.R. Cheeseman, T. Keith, G.A. Petersson, J.A. Montgomery, K. Raghavachari, M.A. Al-Laham, V.G. Zakrzewski, J.V. Ortiz, J.B. Foresman, C.Y. Peng, P.Y. Ayala, W. Chen, M.W. Wong, J.L. Andres, E.S. Replogle, R. Gomperts, R.L. Martin, D.J. Fox, J.S. Binkley, D.J. Defrees, J. Baker, J.P. Stewart, M. Head-Gordon, C. Gonzalez, J.A. Pople, Gaussian, Inc., Pittsburgh PA, 1995.
[30] O. Hübner, V. Termath, A. Berning, J. Sauer, Chem. Phys. Lett. 294 (1998) 37.
[31] S.G. Lias, J.E. Bartmess, J.F. Liebman, J.L. Holmes, R.D. Levin, W.G. Mallard, Gas Phase and Ion Neutral Thermochem., J. Phys. Chem. Ref. Data 17 (1988) Suppl. 1.
[32] B.A. Rumpf, C.E. Allison, P.J. Derrick, Org. Mass. Spectrom. 21 (1986) 295.
[33] For an instrument with much higher resolution, see: A.G. Brenton, C.M. Lock, Rapid Commun. Mass Spectrom. 11 (1997) 1155.
[34] M. Hargittai, N.Y. Subbotina, M. Kolonits, A.G. Gershikov, J. Chem. Phys. 94 (1991) 7278.
[35] S.M. McCullough, A.D. Jones, C.B. Lebrilla, Int. J. Mass Spectrom. Ion Processes 107 (1991) 545.
[36] P. Dai, S. McCullough-Catalano, M. Boulton, A.D. Jones, C.B. Lebrilla, Int. J. Mass Spectrom. Ion Processes 144 (1995) 67.
[37] S. McCullough-Catalano, C.B. Lebrilla, J. Am. Chem. Soc. 115 (1993) 1441.
[38] A.I. Boldyrev, M. Gutowski, J. Simons, Acc. Chem. Res. 29 (1996) 497.
[39] M. Kolbuszewski, J.S. Wright, R.J. Buenker, J. Chem. Phys. 102 (1995) 7519.
[40] C. Heinemann, D. Schröder, H. Schwarz, J. Phys. Chem. 99 (1995) 16195, and references therein.
[41] L.A. Curtiss, P.C. Redfern, K. Raghavachari, J.A. Pople, J. Chem. Phys. 109 (1998) 42, and references therein.